Table VI. Photostabilities

compound	irradiatn time to get a 50% reduction of the initial compd concn, h/min	photodegradation velocity,[a] (mol L^{-1} h^{-1}) × 10^6
5	11/43	1.62
Tinuvin P	17/02	
7	47/05	0.46
6	3/55	4.29[b]
8	3/40	8.98[b]
9	4/10	5.18
10	2/56	11.75

[a] Expressed in molarity diminution with irradiation time. Calculated from the slope of the relationship of absorbance versus irradiation time and conversion to concentration units. [b] The inversion of the photodegradability order is due to the difference between the molar absorption coefficients of both compounds.

studied in this investigation was found to be as follows: phenol **7** > Tinuvin P > phenol **5** >>> ether **9** > ether **6** ≥ phenol **8** > ether **10**. This order is clearly related to the possibility of forming an intramolecular O—H···N hydrogen bond (IMHB).

Conclusions

1-H-3-(2′-hydroxyphenyl)pyrazole (**5**) and 1-methyl-3-(2′-hydroxyphenyl)pyrazole (**7**), which each possess an IMHB linking their phenol proton with the pyrazole N2 lone pair, are photostable. In the first excited singlet state, significant conjugation exists between the two rings of the molecule and therefore rotation about the central carbon–carbon bond is restricted.

These derivatives show proton transfer in the first excited singlet; i.e., their behavior in this regard is different from that of *N*-(2′-hydroxyphenyl)pyrazoles. The existence of an IMHB provides UV stability independently of whether the proton is transferred or not.

Experimental evidence proves that the phosphorescence of compounds **5** and **7** is produced by the nontransferred form. Proton transfer does not occur in the triplet state.

Finally, 1-methyl-5-(2′-methoxyphenyl)pyrazole (**10**) is nonplanar in the ground state but becomes planar in the excited state. The fluorescence emission occurs in the range of 300–340 nm with a good quantum yield. The photophysical properties of this compound suggest that it might behave as an excellent laser dye in the ultraviolet region.

Acknowledgment. We are greatly indebted to CICYT of Spain for financial support (project PB87-0094-C02). Two of us (M.D.S.M. and F.F.) thank the Ministry of Education (MEC) and the Comunidad de Madrid of Spain for two FPI grants. Tinuvin P has been kindly supplied by Ciba-Geigy. Fruitful discussions with Dr. J. F. K. Wilshire have been of the utmost importance in preparing this manuscript.

Registry No. **1**, 118-93-4; **2**, 579-74-8; **3**, 87059-79-8; **4**, 140226-33-1; **5**, 34810-67-8; **6**, 59843-63-9; **7**, 123532-18-3; **8**, 123532-22-9; **9**, 140226-34-2; **10**, 140226-35-3.

Supplementary Material Available: Table of ^1H NMR ^3J (between pyrazole protons) coupling constant values in different solvents, tables of final atomic coordinates, anisotropic thermal factors, and hydrogen parameters for compounds **5**, **7**, and **8**, Figure A of the first UV absorption band of compounds **5–10** in CyH, EtOH, ACN, and DMSO, and Figure B showing the changes in absorbance as a function of ultraviolet exposure for CyH solutions of Tinuvin P and derivatives **5–10**, during the initial 8 h of irradiation (14 pages); listing of observed and calculated structure amplitudes (24 pages). Ordering information is given on any current masthead page.

Intermolecular π Electron Interactions Made Visible. Correlation of Ground- and Excited-State Interactions with Specific Photoreactivities of Isomorphously Crystallized Isoelectronic Compounds[1]

Ingo Ortmann,[†] Stefan Werner,[‡] Carl Krüger,*[,‡] Siegfried Mohr,[§] and Kurt Schaffner*[,†]

Contribution from the Max-Planck-Institute für Kohlenforschung und Strahlenchemie, D-4330 Mülheim a. d. Ruhr, Germany. *Received November 18, 1991*

Abstract: Solid-state UV irradiation of crystalline 4-acetoxy-6-styryl-α-pyrone **1b** yields [2π + 2π] dimers of different constitutions (**2b**, 26%; **3b**, 30%) at 69% conversion of **1b**. This dichotomy is a consequence of the crystal topology of **1b**, which contains two topochemically relevant reaction centers, each composed of two monomers arranged at a center of inversion. In contrast, the isomorphously crystallized isoelectronic 4-acetoxy-6-styryl-1,5-oxazinone **4** is photostable. The electronic properties of **1b** and **4** in the ground and excited states correlate with this difference in photoreactivity. Pyrone **1b** exhibits monomer and excimer fluorescence emission in dilute solution and in the crystal, respectively, whereas the oxazinone **4** under both conditions shows solely monomer fluorescence. Furthermore, the electron deformation density (EDD) of **1b**, determined by the X-X method (the resolution is such that the lone pairs at all heteroatoms of **4** and the localization of the styryl C=C double bond are distinctly visible), shows that the main axes of the nonspheric elongation of positive EDD contour lines are turned from right angles to the molecular plane in order to avoid repulsive π–π interactions. This indicates intermolecular π–π electron interaction between the two reacting double bonds of neighboring molecules of **1b**. The corresponding contour lines of the photostable oxazinone **4** do not show any such distortion. Multipole expansions of the atoms in the crystal structure analyses are in agreement with the results obtained from standard structural refinement.

Solid-state [2π + 2π] photocycloaddition of the naturally occurring 5,6-dehydrokawain (the 4-methoxy-6-styryl-α-pyrone, **1a**) has been reported to yield the unsymmetric dimer **2a**, which has also been isolated from the higher fungi *Aniba gardneri* and

[†] Strahlenchemie.
[‡] Kohlenforschung.
[§] Institut für Organische Chemie, Universität Kiel, D-2300 Kiel, Germany.

(1) Taken in part from Ortmann, I. Ph.D. Thesis, Max-Planck-Institute für Kohlenforschung und Strahlenchemie, Mülheim a. d. Ruhr, and Bergische Universität, Wuppertal, Germany 1991.

0002-7863/92/1514-5048$03.00/0

Table I. Angles and Distances of the Double Bonds Geometrically Suited for Photoreaction and Angles between the Main Molecular Planes and Reaction Planes (α) in the Crystals of **1b** and **4**[a]

1b				**4**			
distance (Å)		angle (deg)		distance (Å)		angle (deg)	
C(8**)-C(5)	4.198 (1)	C(7**)-C(8**)-C(5)	51.3 (1)	C(8**)-N(5)	4.096 (1)	C(7**)-C(8**)-N(4)	56.4 (1)
C(7**)-C(6)	4.217 (1)	C(8**)-C(7**)-C(6)	128.7 (1)	C(7**)-C(6)	4.072 (1)	C(8**)-C(7**)-C(6)	123.0 (1)
		α	73			α	70
C(7)-C(8*)	3.979 (1)	C(8)-C(7)-C(8*)	62.8 (1)	C(7)-C(8*)	4.024 (1)	C(8)-C(7)-C(8*)	60.7 (1)
C(8)-C(7*)	3.979 (1)	C(7)-C(8)-C(7*)	117.2 (1)	C(8)-C(7*)	4.024 (1)	C(7)-C(8)-C(7*)	119.3 (1)
		α	88			α	90

[a] See Figure 1.

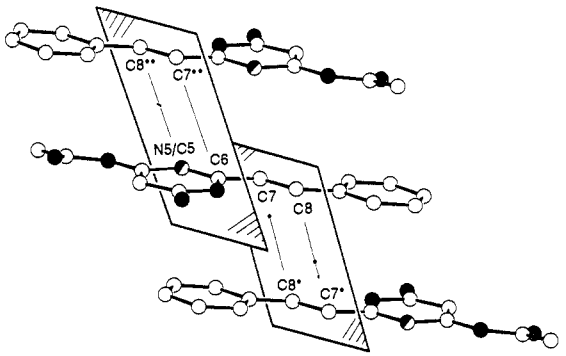

Figure 1. ORTEP presentation of the crystal packing of **1b** and **4**. The photoreacting double bonds are designated as "reaction planes" (note that these planes are best planes; maximum deviation 0.01 Å).

Scheme I

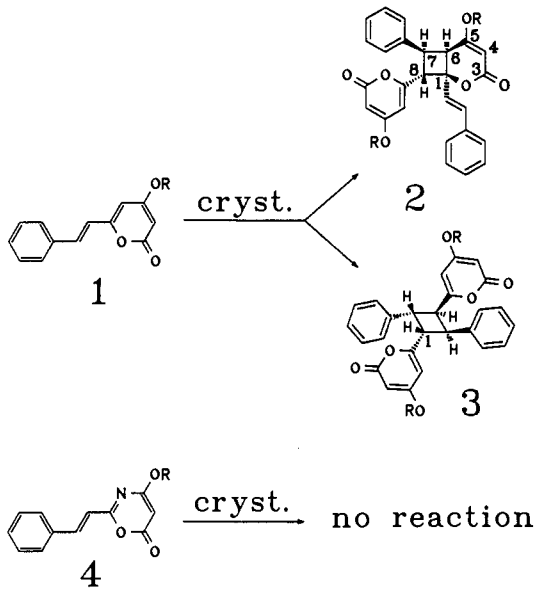

a: R = CH_3

b: R = $COCH_3$

c: R = H

Polygonum nudosum, in addition to a symmetrical dimer (Scheme I).[2,3] We now report on a correlation of ground- and excited-state interactions with specific photoreactivities of two isomorphously crystallized isoelectronic compounds, the 4-acetoxy-6-styryl-α-pyrone **1b** and the corresponding oxazinone **4**.

Table II. Data of the Crystal Structure Determinations of **1b** and **4**

	1b	**4**
empirical formula	$C_{15}H_{12}O_4$	$C_{14}H_{11}NO_4$
mol weight	256.3	257.2
crystal color	yellow	yellow
crystal system	monoclinic	monoclinic
crystal size, mm	0.40 × 0.25 × 0.30	0.33 × 0.33 × 0.33
space group	$P2_1/c$ (No. 14)	$P2_1/c$ (No. 14)
a, Å	9.383 (1)	9.186 (1)
b, Å	13.026 (2)	13.233 (1)
c, Å	10.028 (1)	9.803 (1)
β, deg	98.75 (1)	96.28 (1)
V, Å^3	1211.4	1184.5
Z	4	4
D_{calcd}, g cm^{-3}	1.41	1.44
μ, cm^{-1}	0.96	1.0
λ (Mo-Kα radiation), Å	0.710 69	0.710 69
F(000), e	536	536
diffractometer	Enraf-Nonius CAD4	
scan mode	ω–2θ	ω–2θ
T, K	100	100
no. measd rflns ($\pm h,\pm k,+l$)	24 138	33 837
R_{av}	0.04	0.02
no. unique rflns	5694	5592
Full Data Refinement		
[(sin θ)/λ] range, Å^{-1}	0.0–0.83	0.0–0.83
no. obsd rflns [$I > 2\sigma(I)$]	3755	4812
no. refined params	220	216
R	0.056	0.045
R_w [$w = 1/\sigma^2(F_o)$]	0.050	0.044
error of fit	2.89	5.11
residual electron density, e Å^{-3}	0.4	0.5
High-Order Refinement		
[(sin θ)/λ] range, Å^{-1}	0.65–0.83	0.65–0.85
no. obsd rflns [$I > 2\sigma(I)$]	1548	2295
no. refined params	172	172
R	0.047	0.040
R_w [$w = 1/\sigma^2(F_o)$]	0.045	0.031
error of fit	1.09	1.32

Multipole Refinement

	1b		**4**	
	a	b	a	b
[(sin θ)/λ] range, Å^{-1}	0.0–0.7		0.0–0.7	
no. obsd rflns [$I > 2\sigma(I)$]	2207		2517	
no. refined params	191	293	188	291
R	0.035	0.032	0.022	0.021
R_w [$w = 1/\sigma^2(F_o)$]	0.037	0.032	0.020	0.018
error of fit	2.75	2.45	3.15	2.94

(2) De M. Rezende, C. M. A.; von Bülow, M. V.; Gottlieb, O. R.; Pinho, S. L. V.; de Rocha, A. I. *Phytochemistry* **1971**, *10*, 3167. Mascarenhas, Y. P.; Gottlieb, O. R. *Ibid.* **1977**, *16*, 301. Mascarenhas, Y. P.; Lana, V. L. P.; von Bülow, M. V.; Gottlieb, O. R. *Acta Crystallogr. B* **1973**, *29*, 1361. Gottlieb, O. R.; Veloso, D. P.; de S. Pereira, M. O. *Rev. Latinoam. Quim.* **1975**, *6*, 188; *Chem. Abstr.* **1976**, *84*, 121592d. Kuroyanagi, M.; Yamamoto, Y.; Fukushima, S.; Uno, A.; Noro, T.; Miyase, T. *Chem. Pharm. Bull.* **1982**, *30*, 1602.

(3) For further solid-state photoreactions of styryl-α-pyrones of type **1**, see: Edwards, R. L.; Mir, I. *J. Chem. Soc. C* **1967**, 411. Kaloga, M.; Christiansen, I. *Z. Naturforsch.* **1981**, *36b*, 505; *Ibid.* **1983**, *38b*, 658. Achenbach, H.; Schaller, E.; Regel, W. *Chem. Lett.* **1982**, 741. Achenbach, H.; Karl, W.; Schaller, E. *Angew. Chem., Int. Ed. Engl.* **1972**, *11*, 434.

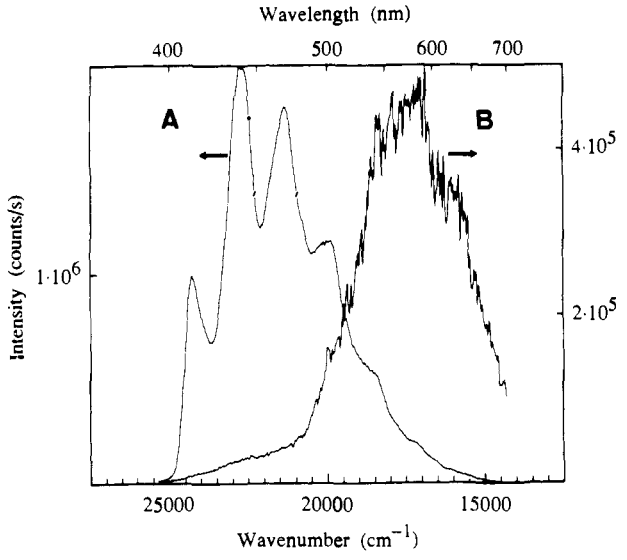

Figure 2. Fluorescence of **1b** in 10^{-5} M ethanol solution (A) and in the crystal (B); 77 K, λ^{exc} = 359 nm.

Results and Discussion

Synthesis of Compounds 1b and 4. The 4-acetoxy-6-styryl-α-pyrone **1b** is readily prepared from **1a**[4] by acid hydrolysis to **1c**[4b,c,5] and esterification with acetyl chloride. The oxazinone analog **4** is available in a one-pot reaction from cinnamoyl isocyanate with excess ketene, comprising a Diels–Alder addition to form the 4-hydroxy-1,5-oxazinone **4c** followed by acetylation.

UV Irradiation of Compounds 1b and 4. Irradiation of the crystalline styryl-α-pyrone **1b** gives [$2\pi + 2\pi$] dimers of different constitutions (**2b** and **3b**, yields 26% and 30%, respectively, at 69% conversion of **1b**). The structures of these compounds are fully established by spectroscopic data (UV, IR, MS, and ^{1}H and ^{13}C NMR; see the Experimental Section).

The unusual dichotomy in the solid-state photochemistry of **1b** can be viewed as a consequence of the crystal topology (Figure 1, Tables I and II),[6] which contains two topochemically relevant reaction centers, each composed of two monomers arranged about an inversion center. The rather long distances between the reacting double bonds and the angular deviations from the ideally 90° arrangement (Table I) are characteristic of the unusually high displacement space of molecules in dichotomic solid-state photoreactions.[7]

Irradiation of **1b** dissolved in various organic solvents led to complex mixtures of products in very low yields, with dimers appearing only in trace amounts in the most concentrated solutions.

The assumption that isoelectronic and isostructural compounds undergo similar solid-state photoreactions has not always been fulfilled in the past.[5] Therefore, it did not appear unusual to us at first when, in contrast to the α-pyrone **1b**, the oxazinone **4**[2] proved photostable. However, the crystal structure analyses reveal the two isoelectronic compounds to form isomorphous crystals; i.e., not only the isolated molecules of **1b** and **4** are similar in their geometry, but so are the crystal packings of the two compounds (Table I). Consequently, the photostability of **4** is not explicable on the basis of geometric considerations alone; rather, electronic factors should be expected to play a decisive role. A first indication was indeed obtained by fluorescence spectroscopy. The emissions of **1b** in dilute solution and in the crystal are characteristic of monomers and excimers, respectively, whereas the oxazinone **4** under both conditions shows solely monomer fluorescence (Figures 2 and 3). In comparison to the solution emission of **1b**, which at low temperature exhibits distinct fine structure, the solid-state fluorescence is strongly red-shifted and nonstructured under all conditions. This is evidently an example of localized excimer formation in the crystal, which has been established in many cases for intermediates on the pathway to solid-state [$2\pi + 2\pi$] photodimerization.[8]

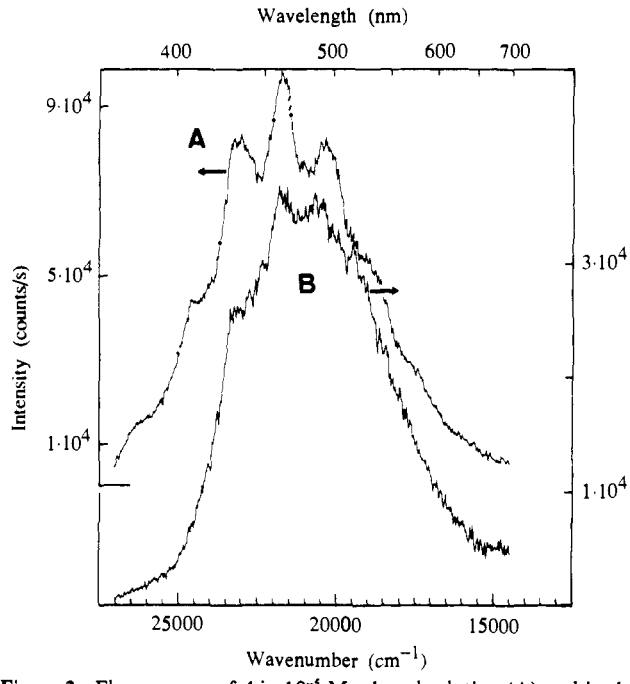

Figure 3. Fluorescence of **4** in 10^{-5} M ethanol solution (A) and in the crystal (B); 77 K, λ^{exc} = 359 nm.

Charge Density Analysis. In the photoreactive pyrone (**1b**), the intermolecular π–π electron interaction is not restricted to the excited state. Interactions between the two reacting double bonds of neighboring molecules can also be established for the ground state by the electron deformation density (EDD) obtained by the X-X method.[9]

The EDD contour lines in the main molecular planes of **1b** and **4** are given in Figure 4. Figure 4B (compound **4**) shows that the C(7)–C(8) double bond is localized, and the lone pairs are clearly visible at N(5), O(1), O(15), O(16), and O(18). The quality of the experimental data, demonstrated by this highly satisfactory resolution, justifies further examination relating to intermolecular interactions. The contour lines of positive EDD within the planes formed by each pair of reactive double bonds of **1b** (which define the "reaction planes"; Figure 1) are clearly distorted, with the main axis of the nonspheric elongation turned from right angles to the molecular plane in order to avoid repulsive intermolecular π–π electron interactions. The EDD distributions in both reaction planes are very similar (Figure 5). In contrast, the contour lines in the expected reaction planes of the photostable oxazinone **4** do not show any distortion (Figure 5D).

Multipole expansions of the atoms[10] in the crystal structure analyses[11] of **1b** and **4** finally permit an interesting juxtaposition (Figure 5: compare B with C and E with F). For each compound, two structure models, a and b, were fitted to the experimental data by least-squares refinement. Model a identifies the molecular plane as an almost ideal mirror plane except for the methyl carbon, but model b does not include this restriction. Model a does not

(4) (a) Dean, M. F. *Naturally Occurring Oxygen Ring Compounds*; Butterworths: London, 1963; p 83. (b) Chmielewska, I.; Cieslak, J.; Gorczynska, K.; Kontnik, B.; Pitakowska, K. *Tetrahedron* **1958**, *4*, 36. (c) Douglas, J. L.; Money, T. *Tetrahedron* **1967**, *23*, 3545.

(5) Macierewicz, Z. *Rocz. Chem.* **1950**, *24*, 144.

(6) A case of multiproduct topochemistry; cf. Kaupp, G.; Frey, H.; Behmann, G. *Chem. Ber.* **1988**, *121*, 2135.

(7) *Organic Solid State Chemistry*; Desiraju, G. R., Ed.; Elsevier: New York, 1987.

(8) Yakhot, V.; Cohen, M. D.; Ludmer, Z. *Adv. Photochem.* **1979**, *11*, 241.

(9) Angermund, K.; Claus, K. H.; Goddard, R.; Krüger, C. *Angew. Chem.* **1985**, *97*, 241; *Angew. Chem., Int. Ed. Engl.* **1985**, *24*, 237.

(10) Hansen, N. K.; Coppens, P. *Acta Crystallogr. A* **1978**, *34*, 909.

(11) Ortmann, I.; Werner, S.; Krüger, C. In *The Application of Charge Density Research to Chemistry and Drug Design*; Jeffrey, G. A., Piniella, J. F., Eds.; NATO ASI Series B250; Plenum Press: New York, 1991; p 365.

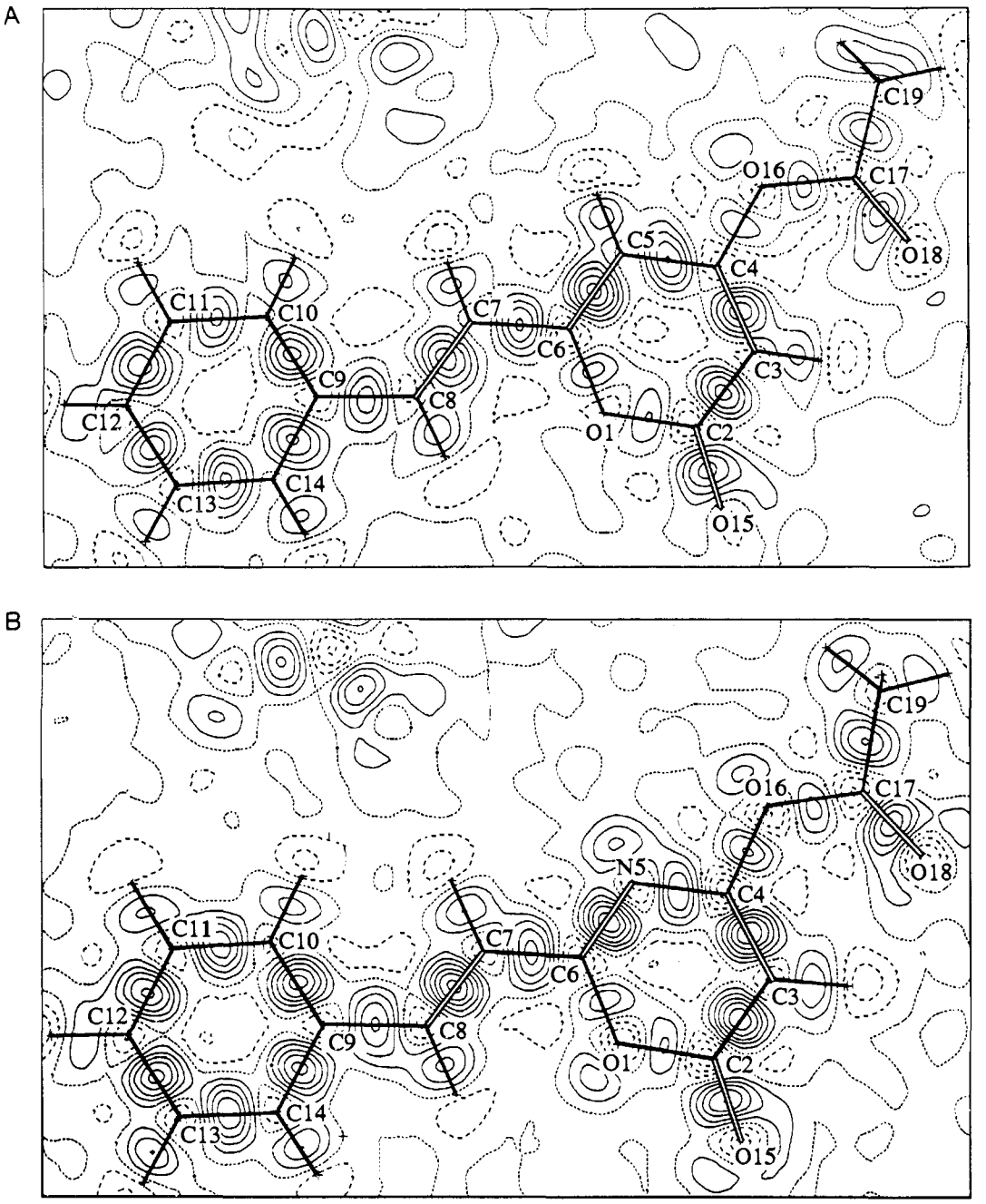

Figure 4. Electron deformation density in the main molecular planes of **1b** (A) and **4** (B).

account for the observed intermolecular effects and, consequently, the EDD[12] of **1b** in the reaction planes (Figure 5B) cannot show any distortion. However, plots mapping the EDD calculated on the basis of model b (Figure 5C) are in agreement with the results obtained from standard structural refinement. In contrast, model a and b contour plots of **4** (Figure 5E,F) do not differ.

The ground- and excited-state π electron interactions in **1b** and **4** are thus correlated, via EDD and fluorescence, with the specific photoreactivities of the isomorphously crystallized isoelectronic compounds. The potential predictive value of such an unprecedented correlation is self-evident. Still, it is difficult to rationalize the EDD distortion within the reaction planes and the connection between this phenomenon and the difference between **1b** and **4** regarding excimer formation. Among the factors which have to be considered are the π electron delocalization as shown by the EDD cuts in the molecular plane (Figure 4), the extent of π–π electron interaction in the two molecules in their ground and excited states, and the electronic configuration in the excited state, viz., π,π* in **1b** vs n,π* (?) in **4**.

Experimental Section

General Methods. Melting points were taken under a microscope on a Kofler hot plate and were not corrected. ^{13}C and ^{1}H NMR spectra were measured on Bruker AM-400 and WH-270 instruments in the FT mode. The chemical shifts are in δ units (with $(CH_3)_4Si$ as internal reference), and the coupling constants (*J*, determined by resolution enhancement) are in hertz; abbreviations are s (singlet), d (doublet), q (quartet), and m (multiplet). IR spectra were run in KBr on a Perkin-Elmer 298 instrument and are given in cm^{-1}. The UV spectra (ethanol) were recorded on Cary 17 and Bruins Omega-10 spectrophotometers; maxima are given in nanometers, with ϵ_{max} values in parentheses. Corrected fluorescence spectra were obtained on a computer-controlled Spex Fluorolog spectrofluorometer.[13] Mass spectra (MS, in *m/z*) were

(12) The EDD was calculated as a Fourier transformation of the difference between structure factors calculated on the basis of the multipole model and structure factors calculated on the basis of the standard spheric atom model.

(13) Holzwarth, A. R.; Lehner, H.; Braslavsky, S. E.; Schaffner, K. *Liebigs Ann. Chem.* **1978**, 2002. Braslavsky, S. E.; Holzwarth, A. R.; Langer, E.; Lehner, H.; Matthews, J. I.; Schaffner, K. *Isr. J. Chem.* **1980**, *20*, 196.

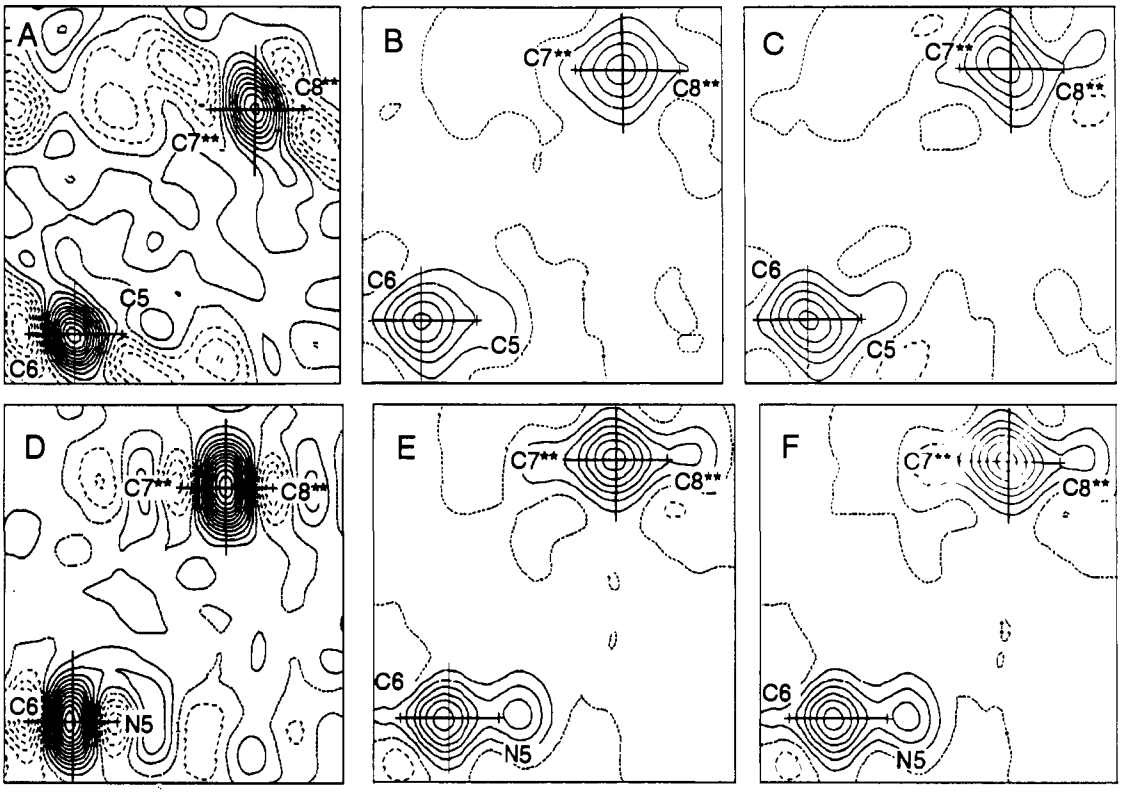

Figure 5. Electron deformation densities in the reaction planes of **1b** leading to the unsymmetric dimer **2** (A–C), after multipole refinement, keeping the molecular mirror plane as a fixed structural element (B), and after multipole refinement without any symmetry restriction (C); D–F are the corresponding cuts of the unreactive compound **4**.

measured on Varian MAT CH5 and Finnigan MAT 8230 instruments at 70 eV. Column chromatography was performed on silica gel 40, 0.04–0.062 mm (Merck). Silica gel Polygram foils Sil G-75 $UV_{254/366}$ (Macherey & Nagel) were used for thin-layer chromatography (TLC); products were spotted either by UV light or with I_2 vapor. The solvents were purified and, when necessary, dried using standard procedures.

Preparation of 4-Acetoxy-6-[(*E*)-2-phenylethenyl]-2*H*-pyran-2-one (1b). A solution of **1a** (6.3 g, 30 mmol; mp 135–136 °C, lit.[4c] mp 137–139 °C) in 50 mL of glacial acetic acid and 50 mL of 48% aqueous HBr was heated to 110 °C for 30 min and then poured onto 400 mL of ice water containing ca. 25 g of $NaHCO_3$. The solution was stirred until the formation of CO_2 had ended. The orange precipitate and the ethyl acetate extract of the mother liquor were combined, dried in vacuo, and washed with cold $CHCl_3$, affording 4.5 g of 4-hydroxy-6-[(*E*)-2-phenylethenyl]-2*H*-pyran-2-one (**1c**, 74% yield): mp 255–256 °C (lit.[5] mp 245–246 °C).

Acetyl chloride (78 mmol) was added dropwise to a stirred suspension of **1c** (4.0 g, 39 mmol) in 90 mL of anhydrous CH_2Cl_2 at room temperature, followed by addition of a solution of triethylamine (10.8 mL, 78 mmol) in 90 mL of CH_2Cl_2. After 30 min the reaction mixture had turned to a clear solution, which was stirred for another 2 h prior to consecutive washing with H_2O, saturated aqueous $NaHCO_3$ solution, and H_2O. After the organic layer was dried over Na_2SO_4 and the solvent was distilled off, the crystalline residue was taken up in toluene–acetone (10:1) and filtered through silica gel. Recrystallization from CH_2Cl_2–CH_3OH gave yellow needles of **1b** (81% yield): mp 128 °C; see Tables I and II for crystal data and Figure 2 for fluorescence; UV 234 (4.12), 241 (4.05), 261 (4.17), 269 (4.19), 359 nm (4.41); IR 1768, 1720, 1635, 1604, 1549, 1182, 1133; ^{1}H NMR (270 MHz, $CDCl_3$) 7.50 + 6.58 (AX, AX, $^3J_{7,8}$ = 16.0, 8- and 7-H, respectively), 7.50–7.24 (AA′BB′C; 5-H_{ar}), 6.10 + 6.08 (AB, $^4J_{3,5}$ = 2.0, 5- and 3-H, respectively), 2.28 (s, 19-H); ^{13}C NMR (68 MHz, $CDCl_3$) 166.8 + 162.9 + 162.7 + 159.6 + 135.0 (5 s, C-17, -4, -2, -6, and C_{ar}, respectively), 136.5 + 118.3 + 102.2 + 102.0 (4 d, C-8, -7, -5, and -3, respectively), 129.7 + 128.9 + 127.5 (3 d, 3 C_{ar}), 21.2 (q, C-19); MS (evaporation at 90 °C) 256 (30, M^+), 214 (40), 170 (24), 145 (28), 131 (19), 103 (25), 77 (29), 43 (100).

Preparation of 4-Acetoxy-6-[(*E*)-2-phenylethenyl]-2*H*-1,5-oxazin-2-one (4). A suspension of cinnamamide (28.2 g, 0.19 mol) in 150 mL of anhydrous 1,2-dichloroethane was treated at room temperature with oxalyl chloride (31.5 g, 0.25 mol). After the initial vigorous release of HCl, the mixture was refluxed for 2 h while the yellow color of the solution changed to deep red. The mixture was then cooled and taken to dryness in vacuo. The solid residue was decomposed in the vacuum at 120–160 °C, and the resulting colorless cinnamoyl isocyanate was distilled at 82–90 °C/(6 × 10^{-2})–(1 × 10^{-1}) Torr (18.6 g, 57% yield). The product was highly sensitive toward moisture: ^{1}H NMR (270 MHz, C_6H_6) 7.40 + 6.13 (AX, $^3J_{2,3}$ = 15.7, 3- and 2-H, respectively), 7.00–6.94 (m, 5 H_{ar}), ^{13}C NMR (68 MHz, C_6H_6) 163.7 + 127.2 (2 s, C-1 and N=*C*=O, respectively), 148.6 + 120.8 (2 d, C-3 and -2, respectively), 133.8 + 131.2 + 129.0 + 128.9 (4 d, 4 C_{ar}).

Ketene (ca. 11 g, 0.26 mol) in 50 mL of anhydrous diethyl ether and cooled to −78 °C was added dropwise under argon to a solution of the isocyanate (15.0 g, 87 mmol) in 200 mL of anhydrous benzene kept at room temperature, followed by stirring for 16 h at room temperature. The solvent was then stripped off in the rotary evaporator, and the residual oil was filtered in toluene–acetone (10:1) through 600 g of silica gel, yielding a yellow powder which gave prisms of **4** on crystallization from benzene–cyclohexane (10:1) (12.4 g, 55% yield): mp 119 °C; see Tables I and II for crystal data and Figure 3 for fluorescence; UV 232 (4.0), 236 (3.99), 254 (3.90), 340 (4.35); IR 1771, 1745, 1630, 1587, 1543, 1365, 1314, 1171, 1128, 1029; ^{1}H NMR (270 MHz, C_6H_6) 7.91 + 6.69 (AX, $^3J_{7,8}$ = 16.1, 8- and 7-H, respectively), 7.58–7.55

Table III. Final Fractional Coordinates of **1b**

atom	*x*	*y*	*z*
O(1)	0.2502 (1)	0.1696 (1)	0.4477 (1)
O(15)	0.2434 (2)	0.3370 (1)	0.4060 (2)
O(16)	0.5080 (2)	0.1079 (1)	0.1606 (1)
O(18)	0.5664 (2)	0.2658 (1)	0.0848 (2)
C(2)	0.2865 (2)	0.2537 (1)	0.3748 (2)
C(3)	0.3724 (2)	0.2356 (1)	0.2699 (2)
C(4)	0.4242 (2)	0.1393 (1)	0.2538 (1)
C(5)	0.3890 (2)	0.0561 (1)	0.3352 (2)
C(6)	0.3010 (2)	0.0737 (1)	0.4288 (1)
C(7)	0.2548 (2)	−0.0051 (1)	0.5140 (1)
C(8)	0.1689 (2)	0.0128 (1)	0.6078 (2)
C(9)	0.1145 (2)	−0.0639 (1)	0.6938 (1)
C(10)	0.1482 (2)	−0.1686 (1)	0.6894 (2)
C(11)	0.0947 (2)	−0.2381 (1)	0.7744 (2)
C(12)	0.0030 (2)	−0.2043 (2)	0.8640 (2)
C(13)	−0.0317 (2)	−0.1013 (2)	0.8686 (2)
C(14)	0.0243 (2)	−0.0315 (1)	0.7855 (2)
C(17)	0.5695 (2)	0.1733 (1)	0.0774 (1)
C(19)	0.6388 (2)	0.1111 (2)	−0.0194 (2)

Table IV. Final Anisotropic Displacement Parameters (ADP) of **1b** (Å²)

atom	$U_{1,1}$	$U_{2,2}$	$U_{3,3}$	$U_{1,2}$	$U_{1,3}$	$U_{2,3}$
O(1)	0.021 (1)	0.017 (1)	0.016 (1)	0.002 (1)	0.007 (1)	0.001 (1)
O(15)	0.038 (1)	0.019 (1)	0.026 (1)	0.006 (1)	0.015 (1)	0.001 (1)
O(16)	0.022 (1)	0.018 (1)	0.019 (1)	−0.002 (1)	0.011 (1)	−0.002 (1)
O(18)	0.024 (1)	0.020 (1)	0.024 (1)	−0.003 (1)	0.009 (1)	0.002 (1)
C(2)	0.021 (1)	0.018 (1)	0.016 (1)	0.002 (1)	0.007 (1)	0.001 (1)
C(3)	0.021 (1)	0.018 (1)	0.016 (1)	0.001 (1)	0.006 (1)	0.001 (1)
C(4)	0.016 (1)	0.018 (1)	0.014 (1)	0.001 (1)	0.005 (1)	−0.001 (1)
C(5)	0.019 (1)	0.017 (1)	0.017 (1)	0.001 (1)	0.008 (1)	0.001 (1)
C(6)	0.017 (1)	0.017 (1)	0.015 (1)	0.001 (1)	0.005 (1)	0.001 (1)
C(7)	0.018 (1)	0.018 (1)	0.017 (1)	0.001 (1)	0.007 (1)	0.002 (1)
C(8)	0.020 (1)	0.017 (1)	0.018 (1)	0.001 (1)	0.007 (1)	0.003 (1)
C(9)	0.018 (1)	0.016 (1)	0.016 (1)	0.001 (1)	0.004 (1)	0.001 (1)
C(10)	0.025 (1)	0.015 (1)	0.024 (1)	−0.002 (1)	0.007 (1)	−0.001 (1)
C(11)	0.029 (1)	0.018 (1)	0.029 (1)	−0.007 (1)	0.006 (1)	0.003 (1)
C(12)	0.027 (1)	0.025 (1)	0.023 (1)	−0.011 (1)	0.003 (1)	0.004 (1)
C(13)	0.022 (1)	0.028 (1)	0.020 (1)	−0.004 (1)	0.007 (1)	0.004 (1)
C(14)	0.022 (1)	0.023 (1)	0.020 (1)	0.002 (1)	0.009 (1)	0.004 (1)
C(17)	0.018 (1)	0.021 (1)	0.017 (1)	−0.003 (1)	0.006 (1)	−0.001 (1)
C(19)	0.028 (1)	0.026 (1)	0.021 (1)	−0.005 (1)	0.013 (1)	−0.004 (1)

Table V. Final Fractional Coordinates of **4**

atom	x	y	z
O(1)	0.2426 (1)	0.6737 (1)	0.0603 (1)
O(15)	0.2499 (1)	0.8389 (1)	0.1021 (1)
O(16)	−0.0177 (1)	0.6063 (1)	0.3527 (1)
O(18)	−0.0785 (1)	0.7575 (1)	0.4432 (1)
N(5)	0.1056 (1)	0.5614 (1)	0.1798 (1)
C(2)	0.2046 (1)	0.7577 (1)	0.1353 (1)
C(3)	0.1145 (1)	0.7376 (1)	0.2430 (1)
C(4)	0.0688 (1)	0.6409 (1)	0.2582 (1)
C(6)	0.1905 (1)	0.5808 (1)	0.0858 (1)
C(7)	0.2372 (1)	0.5006 (1)	−0.0002 (1)
C(8)	0.3265 (1)	0.5167 (1)	−0.0980 (1)
C(9)	0.3826 (1)	0.4403 (1)	−0.1863 (1)
C(10)	0.3452 (1)	0.3377 (1)	−0.1808 (1)
C(11)	0.4029 (1)	0.2685 (1)	−0.2674 (1)
C(12)	0.4999 (1)	0.3000 (1)	−0.3589 (1)
C(13)	0.5382 (1)	0.4015 (1)	−0.3647 (1)
C(14)	0.4789 (1)	0.4708 (1)	−0.2798 (1)
C(17)	−0.0841 (1)	0.6664 (1)	0.4422 (1)
C(19)	−0.1603 (1)	0.6007 (1)	0.5356 (1)

(*AA'XX'*C) + 7.43–7.41 (AA'*XX'C*, 5 H_{ar}), 6.03 (s, 3-H), 2.33 (s, 19-H_3); ^{13}C NMR (68 MHz, C_6H_6) 166.3 + 164.7 + 163.9 + 159.6 + 133.6 (5 s, C-17, -6, -4, -2, and C_{ar}, respectively), 145.2 (d, C-8), 131.0 + 128.9 + 128.2 (3 d, 3 C_{ar}), 117.3 + 95.0 (2 d, C-7 and -3, respectively), 21.0 (q, C-19); MS (evaporation at 90 °C) 257 (19, M^+), 215 (72), 187 (29), 159 (20), 145 (53), 131 (96), 103 (71), 69 (18), 77 (49), 51 (18), 43 (100).

Irradiation. Solutions of **1b** in various organic solvents and concentrations were irradiated for extended periods with the full light of a high-pressure Hg lamp. In all cases, only diffuse product patterns in low yields were shown by TLC. Traces of dimers only appeared in the most concentrated solutions. No attempt was made to identify any of the photoproducts.

In the solid-state irradiation, a suspension of **1b** (2.0 g, 7.8 mmol) in 100 mL of water with an added drop of detergent (Pril) was exposed for 2 h with stirring to the full light of an HPK high-pressure Hg lamp (125 W). The crystals were then filtered off, washed with water, and dried in a desiccator. Chromatography in toluene–acetone (10:1) over 250 g of silica gel gave three fractions: (i) starting material (**1b**, 0.62 g, 31%), (ii) colorless needles of *rel*-(1*R*,6*S*,7*S*,8*S*)-5-acetoxy-7-phenyl-8-(4-acetoxy-2-oxo-2*H*-pyran-6-yl)-1-[(*E*)-2-phenylethenyl]-2-oxabicyclo-[4.2.0]octa-4-en-3-one (**2b**, 0.36 g, 18% yield) from anhydrous ethanol, and (iii) transparent needles of *r*-1,*t*-3-bis[4-acetoxy-2-oxo-2*H*-pyran-6-yl]-*c*-2,*t*-4-diphenylcyclobutane (**3b**, 0.42 g, 21% yield) from anhydrous ethanol.

2b: mp 193 °C; UV 250 (4.48), 248 (3.95), 293 (3.92), 302 (shoulder, 3.88); IR 1780, 1723, 1628, 1567, 1365, 1294, 1180, 1148, 1130, 1014; ^1H NMR (400 MHz, C_6D_6–acetone-d_6, 1:1) 7.45–7.41 + 7.35–7.31 (2 *AA'BB'*C, 4 H_{ar}), 7.23–7.11 (2 AA'*BB'C*, 6 H_{ar}), 7.00 + 6.75 (AB, $^3J_{1^1,1^2}$ = 15.9, 1^2- and 1^1-H, respectively), 6.32 (d, $^4J_{4,6}$ = 1.0, 4-H), 6.17 + 5.93 (AB, $^4J_{8^3,8^5}$ = 2.0, 8^5- and 8^3-H, respectively), 4.64 (d) + 4.37 (dd) + 3.79 (dd, AMX, $^4J_{4,6}$ = 1.0, $^3J_{6,7}$ = 9.1, $^3J_{7,8}$ = 11.7, 8-, 7-, and 6-H, respectively), 1.91 + 1.36 (2 s, 8^4- and 5-OCOCH_3, respectively); ^{13}C NMR (100 MHz, C_6D_6–acetone-d_6, 1:1) 166.5 + 166.1 (2 s, 5- and 8^4-O*C*OCH$_3$), 162.7 + 162.5 + 162.0 + 160.6 + 159.3 + 79.6 (6 s, C-3, -8^2, -8^4, -5, $-8'$, and -1, respectively), 135.3 + 134.5 (2 s, C_{ar}), 132.2 + 123.6 + 103.2 + 102.3 (4 d, C-1^2, -1^1, -8^3, and -8^5, respectively), 128.8/128.7 + 128.4/128.1 + 127.7/126.8 (6 d, *m*/*m*-, *p*/*p*-, and *o*/*o*-C_{ar}, respectively), 106.7 + 53.8 + 44.9 + 39.1 (4 d, $^1J_{CH}$ = 174.7, 137.4, 148.9, and 139.9, respectively, C-4, -8, -6, and -7, respectively), 21.1 + 20.6 (2 q, 5- and 8^4-OCO*C*H$_3$); MS (evaporation at 175 °C) 426 (2),

Table VI. Final Anisotropic Displacement Parameters (ADP) of **4** (Å²)

atom	$U_{1,1}$	$U_{2,2}$	$U_{3,3}$	$U_{1,2}$	$U_{1,3}$	$U_{2,3}$
O(1)	0.021 (1)	0.015 (1)	0.016 (1)	−0.002 (1)	0.008 (1)	−0.001 (1)
O(15)	0.037 (1)	0.016 (1)	0.025 (1)	−0.006 (1)	0.015 (1)	0.001 (1)
O(16)	0.021 (1)	0.016 (1)	0.018 (1)	0.002 (1)	0.010 (1)	0.001 (1)
O(18)	0.024 (1)	0.017 (1)	0.023 (1)	0.003 (1)	0.009 (1)	−0.001 (1)
N(5)	0.019 (1)	0.016 (1)	0.016 (1)	0.001 (1)	0.008 (1)	−0.001 (1)
C(2)	0.022 (1)	0.015 (1)	0.015 (1)	−0.002 (1)	0.006 (1)	0.001 (1)
C(3)	0.022 (1)	0.016 (1)	0.015 (1)	−0.001 (1)	0.006 (1)	0.001 (1)
C(4)	0.016 (1)	0.015 (1)	0.013 (1)	0.001 (1)	0.005 (1)	0.001 (1)
C(6)	0.016 (1)	0.016 (1)	0.014 (1)	0.001 (1)	0.005 (1)	−0.001 (1)
C(7)	0.019 (1)	0.017 (1)	0.017 (1)	−0.001 (1)	0.007 (1)	−0.002 (1)
C(8)	0.019 (1)	0.016 (1)	0.016 (1)	−0.001 (1)	0.006 (1)	−0.002 (1)
C(9)	0.016 (1)	0.016 (1)	0.014 (1)	−0.001 (1)	0.004 (1)	−0.001 (1)
C(10)	0.023 (1)	0.014 (1)	0.021 (1)	0.001 (1)	0.008 (1)	0.001 (1)
C(11)	0.028 (1)	0.016 (1)	0.025 (1)	0.004 (1)	0.009 (1)	0.001 (1)
C(12)	0.024 (1)	0.020 (1)	0.020 (1)	0.006 (1)	0.006 (1)	−0.002 (1)
C(13)	0.021 (1)	0.023 (1)	0.018 (1)	0.001 (1)	0.008 (1)	−0.002 (1)
C(14)	0.021 (1)	0.019 (1)	0.018 (1)	−0.003 (1)	0.009 (1)	−0.002 (1)
C(17)	0.017 (1)	0.018 (1)	0.016 (1)	0.003 (1)	0.006 (1)	0.001 (1)
C(19)	0.027 (1)	0.022 (1)	0.022 (1)	0.005 (1)	0.014 (1)	0.005 (1)

384 (1.8), 341 (1.3), 256 (49), 214 (56), 170 (21), 145 (26), 69 (23), 43 (100).

3b: mp 194-195 °C; UV (302 (3.33); IR 1779, 1724, 1639, 1565, 1407, 1365, 1179, 1014; ^{1}H NMR (400 MHz, $CDCl_3$) 7.31-7.18 (2 AA'BB'C, 10 H_{ar}), 5.92 + 5.85 (AB, $^4J_{1^3,1^5}$ = 2.0, 1^5- and 1^3-H, respectively), 4.48-4.43 + 4.32-4.28 (AA'BB', 4 $H_{cyclobutane}$), 2.20 (s, 1^4- and 3^4-OCOCH_3); MS (evaporation at 185 °C) (pos CI) 530 (10, $M^+ + NH_4$), 462 (1.4), 420 (2.5), 274 (100, $M^+/2 + NH_4$), 137 (21), 120 (25).

Solid-state irradiation of the oxazinone **4** in aqueous suspension as described above did not lead to any photoreaction (analysis by IR and powder diagrams).

X-ray Data Collection, Data Processing, and Structure Refinements. Data for compounds **1b** and **4** were collected on an Enraf-Nonius CAD4 diffractometer equipped with a graphite monochromator. The experimental procedures were similar for both compounds. Pertinent experimental details are given in Table II. Suitable crystals of both compounds were sealed under argon in glass capillaries and kept at 100.0 (5) K during data collection. Cell constants were obtained from 75 (50) automatically centered reflections with $17.68 < 2\theta < 41.04°$ (**1b**) and $24.0 < 2\theta < 40.70°$ (**4**). Three standard reflections were used to monitor intensity fluctuations during measurement. The orientation matrices were established by least-squares refinement using 25 reflections in each case. Three of these reflections were used to record changes in the orientation of the crystals. Deviations in θ larger than 0.12° were followed by calculation of new orientation matrices. All data below $\theta = 20°$ were measured at 7 different Ψ angles in order to detect and minimize the effects of double reflections.[9] For all other reflections, two different Ψ settings (0°, 15°) were used. In addition, for both compounds half-spheres of reciprocal space were recorded. Strong reflections were remeasured at reduced tube power and scaled accordingly during data reduction using three standard reflections. Erroneous measurements were detected with an initial screening process (program PSICOM).[14]

The initial structure models were taken from room-temperature structural investigations. The structures were solved using direct methods (SHELXS-86).[15] Subsequent calculations were performed as described using the low-temperature data sets. Full-matrix least-squares refinements were carried out using a local (GFMLX) modification of ORFLS.[16] All hydrogen atom positions were determined from difference Fourier syntheses. Full data refinement ($(\sin\theta)/\lambda < 0.85$ Å^{-1}) included one scale factor, positional parameters for each atom, and ADP (atomic displacement parameters) for all non-hydrogen atoms. In order to obtain positional parameters and ADP unaffected by the valence electron densities, non-hydrogen atom parameters and the scale factors were refined on the basis of high-order data (see Table II). All refinements were based on F, and the weighting scheme applied was $\sigma^{-2}(F)$. Final high-order parameters are listed in Tables III-VI.

Standard atomic parameters of the heavier atoms were kept fixed during the subsequent multipole refinement. Hydrogen atom positions were refined to correct for the aspherical shift. The multipole structure model was designed for refinement with the program MOLLY.[10] Atomic scattering factors were taken from the literature.[17]

The multipole expansion was terminated at the octopole level for all non-hydrogen atoms. For each hydrogen atom, one dipole oriented in the direction of the C-H bonds was included. Its population was set to 0.2 electron and kept fixed during refinement. Constraints due to chemical equivalence and local site symmetry were used to maintain a reasonable ratio of observed reflections to refined parameters.[18] Radial shielding parameters κ were included in the refinement procedures. For the hydrogen atoms of **1b** this value was set to 1.144, and it was not refined subsequently.[19] The refinements of the multipole models were based on F, and the weighting scheme applied was $\sigma^{-1}(F)$; for further details, see Table II.

Acknowledgment. Part of this work was supported by the Fonds der Chemischen Industrie. I.O. thanks the Volkswagen-Stiftung for a doctoral fellowship.

Registry No. 1b, 138744-79-3; **2b**, 138744-80-6; **3b**, 138744-81-7; **4b**, 138744-82-8.

Supplementary Material Available: Tables of detailed information on the crystal structure determinations, final atomic position parameters, final thermal parameters, and interatomic distances and angles for **1b** and **4** (22 pages); listing of observed and calculated structure factors (36 pages). Ordering information is given on any current masthead page.

(14) PSICOM: program library of X-ray laboratory, MPI für Kohlenforschung.

(15) Sheldrick, G. M. In *Crystallographic Computing*; Sheldrick, G. M., Krüger, C., Goddard, R., Eds.; Clarendon Press: Oxford, 1985; Vol. 3, p 175.

(16) Busing, W. R.; Martin, K. O.; Levy, H. A. *ORNL-TM-305*; Oak Ridge National Laboratory: Oak Ridge, TN, 1962.

(17) *International Tables for X-ray Crystallography*; Ibers, J. A., Hamilton, W. C., Eds.; The Kynoch Press: Birmingham, England, 1974; Vol. IV, p 102.

(18) The corresponding multipole functions at the phenyl carbon atoms were constrained during the refinement procedures. In addition, model a assumed local mm2 symmetry within the phenyl substituent and local 3m symmetry at the methyl carbon atom. The corresponding multipole parameters were constrained for all hydrogen atoms.

(19) Brown, A. S.; Spackman, M. A. *Acta Crystallogr.* **1991**, *A47*, 21.

Chemistry and Kinetics of Singlet (Pentafluorophenyl)nitrene

Russell Poe, Karlyn Schnapp, Mary J. T. Young, Jennifer Grayzar, and Matthew S. Platz*

Contribution from The Ohio State University, Department of Chemistry, 120 West 18th Avenue, Columbus, Ohio 43210. *Received November 14, 1991. Revised Manuscript Received February 24, 1992*

Abstract: The chemistry and kinetics of singlet (pentafluorophenyl)nitrene were studied by chemical trapping and laser flash photolysis techniques. Photolysis of pentafluorophenyl azide in cyclohexane, benzene, diethylamine, pyridine, tetramethylethylene, tetrahydrofuran, dimethyl sulfoxide, and dimethyl sulfide forms adducts in fair to good yields. At ambient temperature singlet (pentafluorophenyl)nitrene is intercepted, and intersystem crossing to the lower energy triplet state is unimportant. Triplet nitrene chemistry can be achieved by benzoylbiphenyl photosensitization, the presence of methanol or ethyl iodide, or by lowering the reaction temperature below 0 °C. The singlet nitrene adduct formed in pyridine is an ylide whose structure has been determined by X-ray crystallography. The ylide has an intense absorption maximum at 390 nm which varies only slightly with solvent. The pyridine ylide is a useful probe for monitoring the absolute kinetics of singlet (pentafluorophenyl)nitrene by laser flash photolysis techniques.

I. Introduction

Light and heat induced decomposition of phenyl azide **1** leads to the formation of polymeric tar along with small amounts of azobenzene and aniline.[1] The yields of the latter two volatile products can be improved by high dilution of phenyl azide.[2] Adducts derived from capture of phenylnitrene **2** are not produced

0002-7863/92/1514-5054$03.00/0